Gianfranco L. Cariolaro (S'60–A'63–M'66) was born in Pozzoleone (Vicenza), Italy, in 1936. He received the degree in electrical engineering and the Libera Docenza in communications from Padova University, Padova, Italy, in 1960 and 1971, respectively.

In 1961 he worked for the Computer Center of Padova University. Since 1962 he has been with the Institute of Electrical and Electronics Engineering, Padova University as Assistant Professor of Electrical Communications and, since 1964, also as Associate Professor of Electronics Components. Currently, he is Associate Professor of Electrical Communications. His main research interests pertain to the statistical aspects of communication engineering and, particularly, to data transmission.

Dr. Cariolaro is a member of the Italian Electrotechnical and Electronic Association. He is Vice-Chairman of the IEEE North Italy Section and Counselor of the IEEE Student Branch of Padova University.

★

Giuseppe P. Tronca was born in Vicenza, Italy, on July 12, 1947. He received the degree in electrical engineering from the University of Padova, Padova, Italy, in July 1972.

Since 1972 he has been working at Telettra Research and Development Laboratories, Vimercate, Italy. His main research interests pertain to the statistical aspects of communication and computer aided design.

Properties of Frame-Difference Signals Generated by Moving Images

DENIS J. CONNOR AND JOHN O. LIMB, SENIOR MEMBER, IEEE

Abstract—**The properties of the frame-difference signals arising from updated "moving" areas and nonupdated "stationary" areas in conditional replenishment interframe encoders are examined. Expressions for the correlation functions and power density spectra of these signals are developed assuming an infinite image field undergoing uniform linear motion. These expressions are modified so as to include the effect of camera integration. Experimentally obtained power spectra are in good agreement with those predicted.**

Three-dimensional frame-difference correlation functions are evaluated using a realistic image correlation function. The properties of the frame-difference correlation functions in directions parallel and perpendicular to the direction of movement, and in the temporal direction are delineated.

It is shown that the correlation function of the frame-difference signal arising from temporally uncorrelated noise is fundamentally different in updated areas compared with nonupdated areas.

I. INTRODUCTION

TELEVISION signals may be used to sense motion in a number of situations—for example, in surveillance, where the need may be to detect any type of movement at all, movement in a particular direction or at a particular speed, or movement of a specific shape. Another example occurs in the frame-to-frame coding of television signals by conditional replenishment [1]–[5]. A moving area detector, or segmenter, separates the moving and stationary areas, and only information about the moving area is transmitted to the receiver. Other examples occur in process control where the position and orientation of a moving object may be important. In all cases the requirements of the detection task will depend upon the specific application and may vary from determining if anything at all in a scene has changed to determining the outline of the moving object. We are interested in conditional replenishment frame-to-frame coders and have a need to specify all parts of the picture that are in motion.

If the input video signal has a high signal-to-noise ratio, then accurate delineation of the moving area is easily achieved using a frame memory. A simple threshold operation on the frame-difference signal suffices [1], [2]. However, in most cases the video signals contain a significant amount of noise and more sophisticated techniques must be used, particularly when the movement is slow [4], [6]. To design these systems we need to be able to characterize the frame differences generated by both movement and noise.[1]

Two distinctly different types of frame-difference signal are considered. In each case a reference frame is stored and the new frame is subtracted from it to obtain the difference signal. In generating the first type of differ-

Paper approved by the Associate Editor for Communication Theory of the IEEE Communications Society for publication without oral presentation. Manuscript received December 28, 1973; revised April 6, 1974.

D. J. Connor was with Bell Laboratories, Holmdel, N. J. 07733. He is now with Bell-Northern Research, Ottawa, Ont., Canada.

J. O. Limb is with Bell Laboratories, Holmdel, N. J. 07733.

[1] See [7] for a study of the probability distribution of frame difference signals.

ence the reference frame is the previous frame and consequently the frame difference signal depends only on the displacement between consecutive frames. In generating the second type of difference the reference frame is brought up to date only for elements which have changed significantly. This type of frame-difference signal occurs when detecting slow movement because a sequence of small differences can build over several frames to become significant. In a conditional replenishment coder the first type of difference signal occurs in moving areas which are continually being updated. The second type of difference signal occurs in nonupdated areas which, if the segmenter is properly designed, correspond to the stationary parts of the picture. Hence, in the following analysis we will refer to the frame-difference signal in the "moving" area (updated reference) and in the "stationary" area (stored reference). As we shall see, the two types of frame-difference signals are markedly different in certain respects.

In this paper we develop expressions for the three-dimensional correlation functions and power density spectra of both types of frame-difference signals, assuming an idealized model for the movement (uniform linear motion). These functions are expressed in terms of the spatial correlation function of the moving object and are broken down into a temporal component plus components parallel to and perpendicular to the direction of motion, thus giving insight into the relative importance of the different dimensions. The theoretical results are compared with measurements of a real-time system in which the conditions closely approximate those of the model.

We assume simple (but reasonably realistic) expressions for the two-dimensional correlation function of the image and noise and hence obtain quantitative comparisons of the various functions. These results are particularly helpful in determining the importance of various operations in practical segmenters.

In the initial analysis we neglect camera effects.[2] However, in Section II-C we incorporate the effect of camera integration on the power spectra of the frame-difference signals, so as to allow comparison of the theoretical and experimental results. As well, in Sections IV-A and IV-B we include the effect of camera integration on the various correlation functions.

Assume that an infinite image field is undergoing a uniform translational movement. If we sample the image field at a uniform rate to produce a sequence of frames, $1,2,3,\cdots, h,\cdots, j,\cdots$, and if a point in the image given by the vector $\boldsymbol{p} = (x,y)$ moves a vector distance $\Delta\boldsymbol{p} = (\Delta x, \Delta y)$ in a frame time T, then the intensity functions for the hth and jth frames are related by

$$i(x,y,jT) = i[x - (j-h)\Delta x, y - (j-h)\Delta y, hT] \tag{1}$$

or

$$i(\boldsymbol{p},jT) = i[\boldsymbol{p} - (j-h)\Delta\boldsymbol{p}, hT] \tag{2}$$

and

$$i(\boldsymbol{p},hT) = i[\boldsymbol{p} + (j-h)\Delta\boldsymbol{p}, jT]. \tag{3}$$

If we assume the intensity function is wide sense stationary and has zero mean, then since the frames are identical except for a translation, they have the same spatial correlation function:

$$I(\boldsymbol{\varrho}) = \langle i(\boldsymbol{p},jT)\cdot i(\boldsymbol{p}-\boldsymbol{\varrho},jT)\rangle, \qquad j = 1,2,\cdots \tag{4}$$

where the vector

$$\boldsymbol{\varrho} = (\alpha,\beta)$$

and $\langle\ \rangle$ denotes a spatial average over x and y. Given these definitions we can proceed with our analysis.

II. CORRELATION FUNCTIONS AND POWER SPECTRA FOR "MOVING" AREA AND "STATIONARY" AREA FRAME-DIFFERENCE SIGNALS

In the following analysis, we develop expressions for the spatial and temporal correlation function and power spectra of the two types of frame-difference signal. In order to distinguish the various functions we will be dealing with, we adopt the following notation: lower case letters refer to the original time and space function; capital letters refer to the corresponding correlation functions; and script letters refer to the power density spectra. The two types of frame-difference functions will be distinguished as follows: for the "moving" areas discussed earlier, the reference frame is continually updated so the functions associated with this type of frame-difference signal will be $u_{\Delta\boldsymbol{p}}$, $U_{\Delta\boldsymbol{p}}$, $\mathcal{U}_{\Delta\boldsymbol{p}}$, where the fact that they are parametrically dependent on the speed and direction of motion ($\Delta\boldsymbol{p}/T$) is explicitly noted by the subscript $\Delta\boldsymbol{p}$. For the "stationary" areas the reference frame is fixed, so the corresponding functions will be denoted as $f_{\delta,\Delta\boldsymbol{p}}$, $F_{\delta,\Delta\boldsymbol{p}}$, $\mathcal{F}_{\delta,\Delta\boldsymbol{p}}$, where δ is the number of frames that have elapsed since the reference was last updated.

A. The "Moving" Area Frame-Difference Signal

In the moving area the frame-difference signal is

$$u_{\Delta\boldsymbol{p}}(\boldsymbol{p},jT) = i(\boldsymbol{p},jT) - i[\boldsymbol{p},(j-1)T] \tag{5}$$

which, by using (3), becomes

$$u_{\Delta\boldsymbol{p}}(\boldsymbol{p},jT) = i(\boldsymbol{p},jT) - i(\boldsymbol{p}+\Delta\boldsymbol{p},jT). \tag{6}$$

The three-dimensional correlation function for the "moving area" frame-difference signal is, by definition,

[2] Most practical cameras degrade a moving picture imaged on the target in at least two ways. First, a point on the target integrates all light falling on it from the time the point is scanned in one frame to the time it is scanned in the next frame. Second, the target may not be completely discharged when it is scanned and some residual signal may be left on the target. The first source of degradation is inherent in the operation of most cameras while the second is quite negligible in high-quality cameras.

$$U_{\Delta \boldsymbol{p}}(\boldsymbol{\varrho},\gamma T) = \langle u_{\Delta \boldsymbol{p}}(\boldsymbol{p},jT)\cdot u_{\Delta \boldsymbol{p}}[\boldsymbol{p}-\boldsymbol{\varrho},(j-\gamma)T]\rangle \quad (7)$$

where

$$\gamma = \cdots -2,-1,0,1,2\cdots.$$

Using (3) and (6) in (7) gives

$$\begin{aligned} U_{\Delta \boldsymbol{p}}(\boldsymbol{\varrho},\gamma T) = \langle & i(\boldsymbol{p},jT)\cdot i(\boldsymbol{p}-\boldsymbol{\varrho}+\gamma\Delta\boldsymbol{p},jT) \\ & - i(\boldsymbol{p},jT)\cdot i[\boldsymbol{p}-\boldsymbol{\varrho}+(\gamma+1)\Delta\boldsymbol{p},jT] \\ & - i(\boldsymbol{p}+\Delta\boldsymbol{p},jT)\cdot i(\boldsymbol{p}-\boldsymbol{\varrho}+\gamma\Delta\boldsymbol{p},jT) \\ & + i(\boldsymbol{p}+\Delta\boldsymbol{p},jT)\cdot i[\boldsymbol{p}-\boldsymbol{\varrho}+(\gamma+1)\Delta\boldsymbol{p},jT]\rangle. \end{aligned} \quad (8)$$

If we take the expected value of each of the terms in (8) and use the correlation of the intensity function as given in (4), we obtain

$$\begin{aligned} U_{\Delta \boldsymbol{p}}(\boldsymbol{\varrho},\gamma T) = & \ 2I(\boldsymbol{\varrho}-\gamma\Delta\boldsymbol{p}) \\ & - \{I(\boldsymbol{\varrho}-(\gamma+1)\Delta\boldsymbol{p}) + I(\boldsymbol{\varrho}-(\gamma-1)\Delta\boldsymbol{p})\}. \end{aligned} \quad (9)$$

Thus (9) is the spatial and temporal correlation function of the "moving area" frame-difference signal in terms of the correlation function of the original image. If desired, one can write $\boldsymbol{\varrho}$, $\boldsymbol{p}$, and $\Delta\boldsymbol{p}$ in terms of horizontal and vertical components to give

$$\begin{aligned} U_{\Delta x,\Delta y}(\alpha,\beta,\gamma T) = & \ 2I(\alpha-\gamma\Delta x,\beta-\gamma\Delta y) \\ & - I[\alpha-(\gamma+1)\Delta x,\beta-(\gamma+1)\Delta y] \\ & - I[\alpha-(\gamma-1)\Delta x,\beta-(\gamma-1)\Delta y]. \end{aligned} \quad (10)$$

In the following we will assume, without loss of generality, that movement is in the x-direction, i.e., $\Delta\boldsymbol{p} = (\Delta x,0)$. When this assumption is made, U and $\mathfrak{U}$ will use the subscript Δx rather than $\Delta\boldsymbol{p}$. Thus, x and α will be parallel to the movement, and y and β will be at right angles to the movement.

Let us now turn to the power density spectrum of the frame-difference signal in the moving area. Let the frequency domain variables corresponding to α, β, and γT be θ, ϕ and ω, respectively, and denote the Fourier transform of U by $\mathfrak{I}(U)$.[3] Now define

$$\mathfrak{U}(\theta,\phi) = \sum_{\omega} \mathfrak{U}(\theta,\phi,\omega) = \mathfrak{I}\{U(\alpha,\beta,0)\} \quad (11)$$

and similarly,

$$\mathfrak{U}(\theta) = \int_{-\infty}^{\infty} \mathfrak{U}(\theta,\phi)\, d\phi = \mathfrak{I}\{U(\alpha,0,0)\} \quad (12)$$

and in the same manner we will define the other power spectra of both u and i.

From (10), using (11), we have

$$\mathfrak{U}_{\Delta x}(\theta,\phi) = \mathfrak{g}(\theta,\phi)\sin^2\frac{\theta\Delta x}{2}. \quad (13)$$

[3] Note that $\mathfrak{I}(U)$ is a Fourier integral transform in θ and ϕ and a discrete Fourier transform in ϕ.

Equation (13) is the spatial power density spectrum of the moving area frame-difference signal. Equation (13) can be further divided into its horizontal and vertical forms to give further understanding of the process.

From (12) and (13) we have

$$\begin{aligned} \mathfrak{U}_{\Delta x}(\theta) &= \sin^2\frac{\theta\Delta x}{2}\int_{-\infty}^{\infty} \mathfrak{g}(\theta,\phi)\, d\phi \\ &= \mathfrak{g}(\theta)\sin^2\frac{\theta\Delta x}{2}. \end{aligned} \quad (14)$$

Similarly, using (10), we have

$$\mathfrak{U}_{\Delta x}(\phi) = \mathfrak{I}[2I(0,\beta) - I(-\Delta x,\beta) - I(\Delta x,\beta)] \quad (15a)$$

and using the symmetry of I,

$$\mathfrak{U}_{\Delta x}(\phi) = \mathfrak{I}\left[2I(0,\beta)\left(1-\frac{I(\Delta x,\beta)}{I(0,\beta)}\right)\right]. \quad (15b)$$

If $I(\alpha,\beta)$ is separable, then

$$\frac{I(\Delta x,\beta)}{I(0,\beta)} = R(\Delta x) \quad (16)$$

where $R(\ )$ is the normalized correlation function of the image signal. Thus

$$\mathfrak{U}_{\Delta x}(\phi) = 2\mathfrak{g}(\phi)[1-R(\Delta x)]. \quad (17)$$

By comparing (14) and (17) we can see the difference between the power spectrum in the same direction as the movement and the power spectrum at right angles to the movement. In the first case the power density of the original signal is *shaped* by the $\sin^2$ function. At very slow speeds (less than 0.5 elements/frame) this is essentially a differentiating operation. However, the power spectrum at right angles to the movement [assuming separability of $I(\alpha,\beta)$] is not changed in shape by the movement but is multiplied by a scaling factor which depends upon the amount of movement.

Similarly, we can obtain the temporal power spectrum by

$$\mathfrak{U}_{\Delta x}(\omega) = \mathfrak{I}[U_{\Delta x}(0,0,\gamma T)] \quad (18$$

and using the symmetry of the correlation function $I(\alpha,\beta)$ we have

$$\mathfrak{U}_{\Delta x}(\omega) = \frac{T}{|\Delta x|}\mathfrak{g}(\omega T/\Delta x)\sin^2\frac{\omega T}{2}. \quad (19$$

Comparing (14) and (19) it is apparent that if one make the substitution $\theta = \omega T/\Delta x$, the two equations are the same except for a scale factor $T/|\Delta x|$.

B. "Stationary" Area Frame-Difference Signal

As described above, the frame-difference signal for "stationary" areas is obtained by taking the difference between the present frame and a fixed reference frame i

the stationary or slowly moving parts of the picture. The frame-difference signal is given by

$$f_{\delta,\Delta p}(p, jT) = i(p, jT) - i[p, (j - \delta)T] \quad (20)$$

where δ is the number of frames between the present frame and the fixed reference frame. Using (3), we obtain

$$f_{\delta,\Delta p}(p, jT) = i(p, jT) - i(p + \delta\Delta p, jT). \quad (21)$$

We cannot proceed as we did for the "moving" area since the statistical properties of $f_{\delta,\Delta p}$ are dependent on δ, and hence the process described by $f_{\delta,\Delta p}$ is temporally nonstationary. However, we can calculate the spatial correlation function

$$F_{\delta,\Delta p}(\varrho) = \langle f_{\delta,\Delta p}(p, jT) \cdot f_{\delta,\Delta p}(p - \varrho, jT) \rangle$$

and using the correlation function of $i(p)$ given in (4), we have

$$F_{\delta,\Delta p}(\varrho) = 2I(\varrho) - I(\varrho - \delta\Delta p) - I(\varrho + \delta\Delta p). \quad (22)$$

If we compare this with the corresponding function for the "moving" area, (9),

$$U_{\Delta p}(\varrho,0) = 2I(\varrho) - [I(\varrho - \Delta p) + I(\varrho + \Delta p)] \quad (23)$$

we see that they differ only in the factor δ that multiplies Δp in (22). Thus given two speeds Δp_1 and Δp_2 related by $\Delta p_2 = \delta(\Delta p_1)$, we have

$$F_{\delta,\Delta p_1}(\varrho) = U_{\Delta p_2}(\varrho,0) = U_{\delta\Delta p_1}(\varrho,0). \quad (24)$$

In other words, the spatial correlation of the frame-difference signal from a slowly moving "stationary" area will be the same as the spatial correlation of the frame-difference signal from a "moving" area that is moving δ times as fast. Because of the similarity of the two expressions (22) and (23) we obtain from (13) the power density for the "stationary" case:

$$\mathcal{F}_{\delta,\Delta x}(\theta,\phi) = \mathcal{I}(\theta,\phi) \sin^2 \frac{\theta\delta\Delta x}{2}. \quad (25)$$

C. The Effect of Camera Integration on the Power Spectra

As mentioned previously, most practical cameras temporally filter the image since they integrate the light falling on the target. This filtering alters the electrical signal so that there need not be a direct correspondence between the spatial distribution of light on the target at a given instant of time and the associated electrical image. For movement at high speeds the filtering action due to target integration is substantial, as we shall see.

To find the point-spread function due to camera integration, assume that a point source of light is moving in a straight line with uniform velocity such that at time t_1 the point is at $p_0 - \Delta p/2$ and one frame later it is at point $p_0 + \Delta p/2$. The resulting image signal will be zero everywhere except along the path traversed by the point source. Thus the point-spread function due to smooth linear motion is an impulse sheet, the length of which is proportional to the distance traveled during one frame time T. Let the energy of the point source in time T be unity, then the point-spread function of the camera is given by

$$g(p) = \begin{cases} \infty, & \text{for all } p = p_0 + a\ \Delta p \text{ with } -1/2 \leq a \leq 1/2 \\ 0, & \text{otherwise.} \end{cases} \quad (26)$$

As before, let Δp be in the horizontal direction, i.e., let $\Delta p = (\Delta x, 0)$. Taking the Fourier transform,

$$G(\theta,\phi) = \frac{\sin \theta\Delta x/2}{\theta\Delta x/2}. \quad (27)$$

Let $i_1(x,y,jT)$ be the image obtained from the camera if there were no target storage and $i_2(x,y,jT)$ be the image resulting when storage occurs. Then, if the power spectra are $\mathcal{I}_1$ and $\mathcal{I}_2$, we have [8]

$$\mathcal{I}_2(\theta,\phi) = \mathcal{I}_1(\theta,\phi) \cdot |\, G(\theta,\phi)\, |^2. \quad (28)$$

We can now use (28) to find the spatial power spectral density of the frame-difference signal in terms of $\mathcal{I}_1$, the equivalent power spectral density of the light incident on the target. Using (28) to substitute in (13) for $\mathcal{I}(\theta,\phi)$, we get

$$\mathcal{U}_{\Delta x}(\theta,\phi) = \mathcal{I}_1(\theta,\phi) \cdot \sin^2 \frac{\theta\Delta x}{2} \left[\sin \frac{\theta\Delta x}{2} \Big/ \frac{\theta\Delta x}{2} \right]^2. \quad (29)$$

To see the effect of target integration, the filter component of (29) due solely to taking frame differences $\sin^2(\theta\Delta x/2)$, is plotted for different values of Δx together with the modified filter component that results when target integration is also incorporated (Fig. 1). At $\Delta x = 0.5$ picture elements/frame (pel), target integration is negligible and the frame differencing is tantamount to spatial differentiation (differentiation corresponds to the straight line asymptote in Fig. 1).

At $\Delta x = 4$ pel the effect of target integration is significant above 0.05 BW where BW is the spatial bandwidth of $i(x,y)$.

The power density spectrum for the "stationary" area frame-difference signal, including camera integration, is obtained by combining (25) and (27):

$$\mathcal{F}_{\delta,\Delta x}(\theta,\phi) = \mathcal{I}(\theta,\phi) \cdot \sin^2 \frac{\theta\delta\Delta x}{2} \left[\sin \frac{\theta\Delta x}{2} \Big/ \frac{\theta\Delta x}{2} \right]^2. \quad (30)$$

Note that the filtering action due to camera integration is not dependent on δ, the number of frames between the present frame and the fixed reference frame, whereas the filtering due to the frame-differencing operation is. Thus, when camera integration is included, the power density spectra from a slowly moving "stationary" area will not be the same as from a "moving" area that is moving δ times as fast [i.e., $\Delta p_2 = \delta(\Delta p_1)$ in (24)] since the effect of temporal filtering will be more pronounced in the latter.

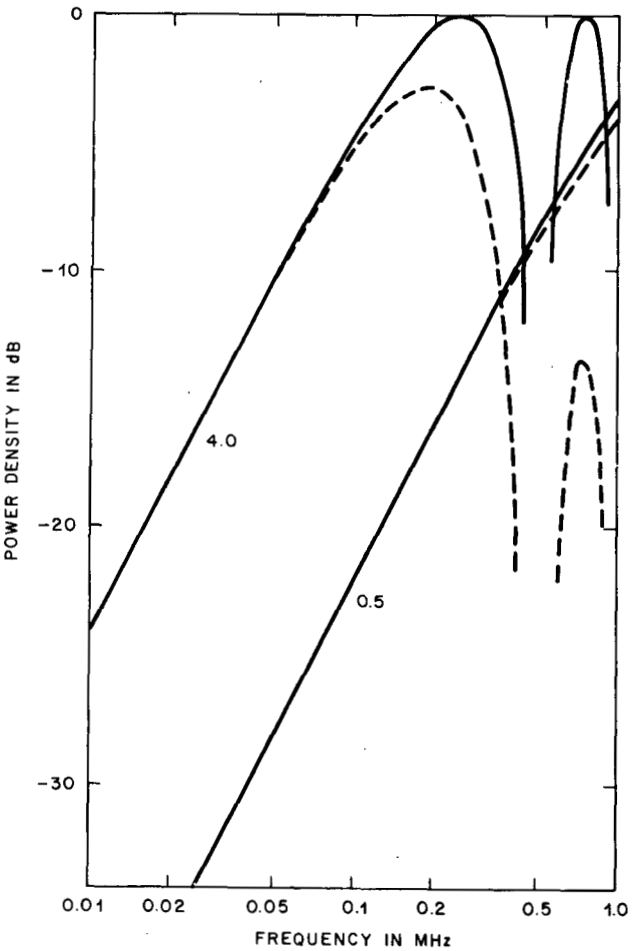

Fig. 1. In obtaining the PDS of the frame-difference signal $\mathfrak{U}_{\Delta z}(\theta)$ the PDS of the video signal is modified by the above functions (29). The full curves are the attenuation due to the frame-to-frame subtraction at speeds of 0.5 and 4.0 pef. The dashed curves, in addition, take into account the effect of camera integration. At low speeds (less than 0.5 pef) the effect of camera integration is negligible and the effect of frame-to-frame subtraction is tantamount to differentiation yielding a function with a slope of 20 dB/decade.

III. MEASUREMENT OF SPECTRA OF FRAME-DIFFERENCE SIGNALS

We measured the power-density spectra of moving images to compare them with the predictious of the previous sections. An attempt was made to simulate as closely as possible the assumptions under which the calculations were made. The camera scene contained an object (a cutout photograph of a head and shoulders) moving with uniform horizontal or vertical speed against a flat background. The object was not "infinite" in extent and hence edge effects modify the results somewhat compared with the theoretical predictions.

A. Recording Equipment

The recording arrangement is shown in Fig. 2. The signal from the video camera is approximately Picturephone® format, that is, a 1-MHz bandwidth, 271 lines/frame, and 30 frames/s with 2:1 interlace. The signal was then digitized at a 2-MHz rate with 8-bit accuracy. A frame memory was connected to take the signal either directly from the input, from a subtractor, or directly from its own output. The frame memory was switched between these three sources at the frame rate in such a manner as to store the required signal in the frame memory. For example, to store a "moving" area frame-difference signal, the switch would be put to position 1 for the duration of one frame so that at the end of one frame the input digital signal would be stored in the frame memory. During the next frame the switch would be moved to position 2 and the signal entering the frame memory would be the frame-difference signal generated by subtracting the signal stored in the frame memory from the input. The switch would then be moved to position 3 and left there, causing the frame-difference signal in the frame memory to continuously circulate in the frame-store loop.

® Registered service mark of the American Telephone and Telegraph Company.

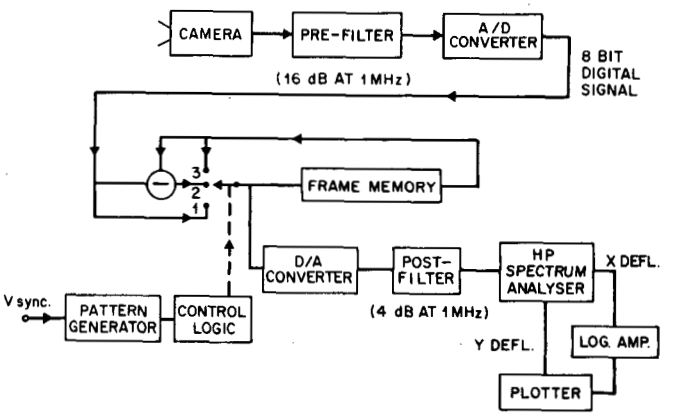

Fig. 2. Block diagram of instrumentation used to record the power density spectra of the video signal and frame-difference signals. The pre- and postfilters were fourth-order maximally flat filters. The Hewlett Packard spectrum analyzer used type 8553B RF plug-in and type 8552B IF plug-in.

A 10-kHz bandpass filter was used in the RF section of the spectrum analyzer, the intention being to purposely attenuate the line frequency components in the signal so that the recorded spectrum was essentially due to horizontal components.

B. Results

The frequency response of the measuring equipment (prefiltered, digitized, and postfiltered) is shown in Fig. 3. It can be seen that the power spectrum falls off very rapidly after 600 kHz, due mainly to the filtering. Also shown in Fig. 3 are the power density spectra (PDS's) of the video signal at speeds of 0.5, 2, and 4 pef (picture elements/frame).[4]

At a speed of 0.5 pef the filtering effect of camera integration is negligible (see Fig. 1) and the spectra falls off with a slope of approximately 31 dB/decade (except for

[4] These spectra would normally contain strong harmonics of the line frequency (8 kHz) due to the blanking interval in the signal and, to a lesser extent, other factors such as shading across the picture. These effects were virtually eliminated by first storing the plain background signal with the moving object removed and then subtracting this signal from the video signal containing the moving object.

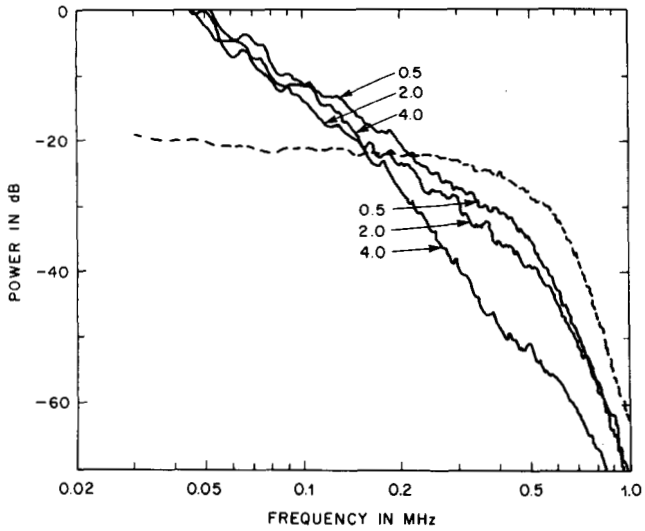

Fig. 3. Power density spectra of the video signal at speeds of 0.5, 2.0, and 4.0 pef. The dashed curve gives the response of the overall system to a signal with a flat PDS. The attenuation at high frequencies is due to the pre- and postfiltering. The effect of camera integration on the video signal at higher speeds is seen in the reduced power at higher frequencies.

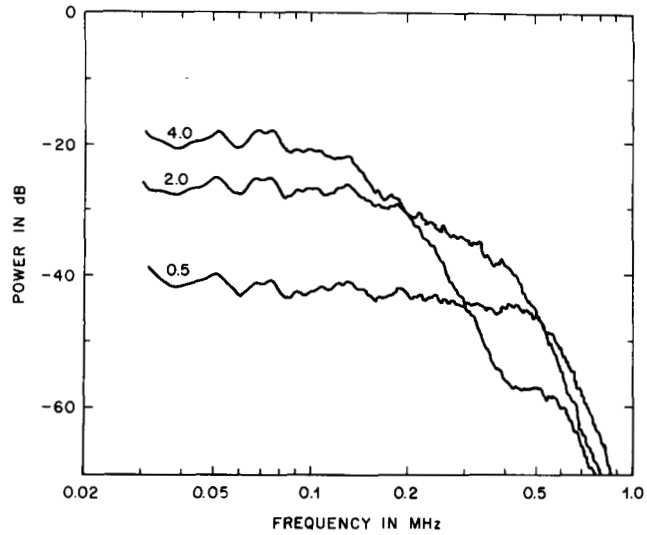

Fig. 4. Power density spectra of the frame-difference signal $\mathfrak{U}_{\Delta x}(\theta)$ at speeds of 0.5, 2.0, and 4.0 pef. Note the increase in power density at low frequencies as the speed increases and the small dip at approximately 0.45 MHz in the curve for a speed of 4 pef.

the high frequencies where the pre- and postfiltering increases the slope). The effect of camera integration is clearly seen in the frequency range above 100 kHz as the speed increases from 0.5 to 4 pef.

At slow speeds the PDS of the frame-difference signal $\mathfrak{U}_{\Delta x}(\theta)$ is essentially flat (Fig. 4). The 31 dB/decade fall in the power density of the video signal is partially cancelled by the 20 dB/decade increase in power density due to the differencing operation (see Fig. 1). For low frequencies where the angle $\theta\Delta x/2$ is small, the amplitude of the frame-difference signal is proportional to frequency (14), and hence one should expect an increase in the PDS of the frame-difference signal of 6 dB as the speed is doubled. Measurements show that the power increased by 7 dB in going from 0.5 to 1, 1 to 2, and 2 to 4 pef, a figure which is within the accuracy of the experimental results.

At a speed of 4 pef we should expect a null in the PDS at 0.5 MHz. A small dip is evident at approximately 0.45 MHz. The small displacement of the null could well be due to inaccuracies in the speed of movement of the moving target and perhaps to a lesser extent in the calibration of the spectra. The peak one would expect at approximately 0.75 MHz is largely masked by the fact that, first, the PDS of the video signal falls very rapidly at high frequencies and, second, the filtering action of the camera produces a further attenuation of approximately 10 dB (see Fig. 9). We will see later that with the "stationary" frame-difference signal the effect of camera integration is less and as a consequence sharper minima and maxima may be obtained.

The element-difference signal and frame-difference signal at a speed of 1 pef are plotted in Fig. 5. From (6) we would expect the two signals to be identical when $\Delta x = 1$ pel and hence the PDS would be the same. In fact, there is a very close correspondence between the spectra.

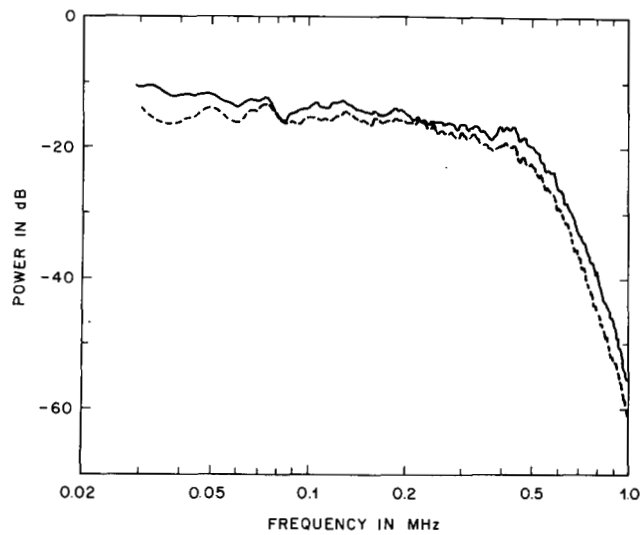

Fig. 5. Comparison of power density spectra of the element-difference signal and the frame-difference signal, both recorded at a speed of 1 pef. The dashed curve is the frame-difference signal $\mathfrak{U}_{\Delta x}(\theta)$.

Equation (17) indicates that the PDS of the vertical-motion frame-difference signal should be a scaled version of the PDS of the video signal. Comparison of the spectra in Fig. 6 indicate that this is not quite borne out by the measurements. The PDS of the vertical-motion frame-difference signal falls off more rapidly than the PDS of the horizontal-motion frame-difference signal but with nowhere near the slope of the video signal. Also, note that, as one would expect, the effect of camera integration at higher frequencies (0.5–0.8 MHz) is less apparent in the PDS of the vertical-motion frame-difference signal.

Fig. 7 shows the PDS of the "stationary" frame-difference signal $\mathfrak{F}_{\Delta x,\delta}(\theta)$ with $\delta = 4$ at a speed of 1 pef. The PDS of the "moving" frame-difference signal at a speed of 4 pef should be similar to this since the displacement between the frames that are being subtracted is the same.

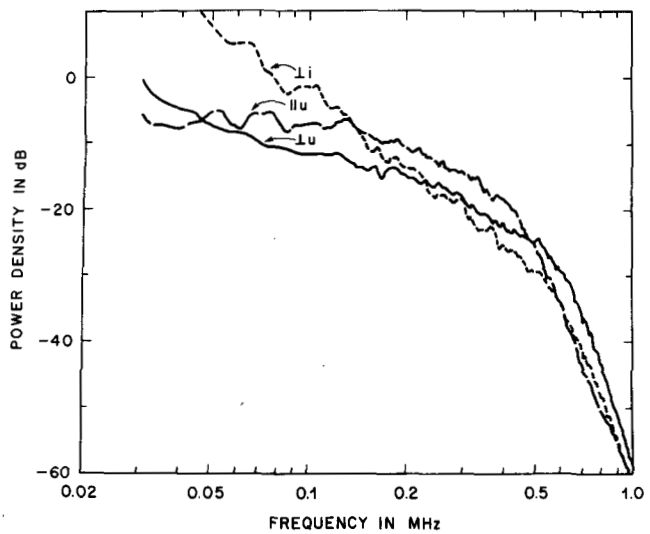

Fig. 6. Comparison of the PDS parallel to and perpendicular to the direction of movement. The PDS for the perpendicular movement (full curve) is steeper at middle and low frequencies than the curve for parallel movement (long dashes) but not as steep as the curve (perpendicular movement) for the video signal (short dashes). All curves were measured at a speed of 2 pef.

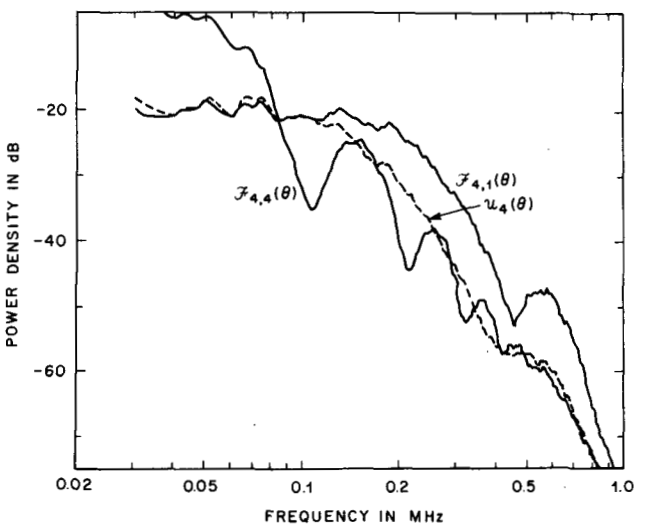

Fig. 7. The power spectrum $\mathcal{F}_{\delta,\Delta x}(\theta)$ with $\delta = 4$ and $\Delta x = 1$ (full curve) has a null at approximately 0.5 MHz which is sharper than the null in the spectrum of $\mathcal{U}_{\Delta x}(\theta)$ with $\Delta x = 4$ (dashed curve) because the effects of camera integration are much less. The curve $\mathcal{F}_{\delta,\Delta x}(\theta)$, with $\delta = \Delta x = 4$ has nulls at multiples of approximately 0.125 MHz.

However, for the stationary frame-difference signal the amount of camera integration is only one-fourth of that occurring in the moving frame-difference signal. The curves are indeed very similar except for the anticipated attenuation at higher frequencies and the less distinct minima and maxima of the "moving" PDS. Also shown in Fig. 7 is the PDS of the "stationary" frame-difference signal at a speed of 4 pef with $\delta = 4$. In this instance the first minima should occur at 0.125 MHz. Camera integration has attenuated the maxima at higher frequencies.

Fig. 8 compares the PDS of the "stationary" frame-difference signal obtained in one case with horizontal movement and in another case with vertical movement. In both instances the speed was 2 pef and $\delta = 4$. It can be

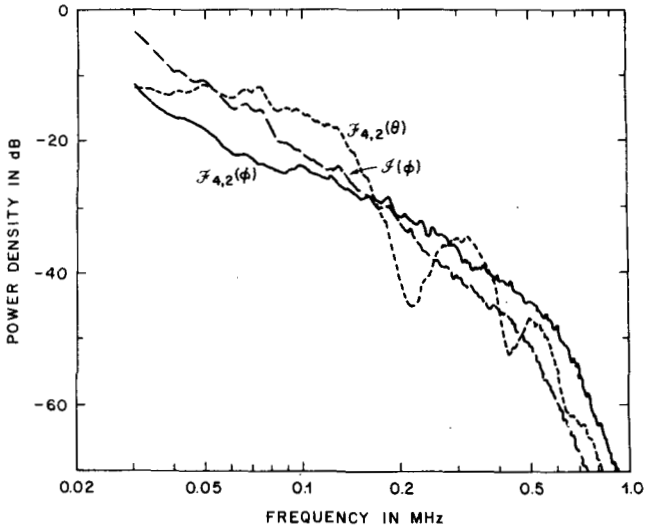

Fig. 8. Comparison of the spectra $\mathcal{F}_{4,2}(\theta)$ (parallel movement, short dashed curve) and $\mathcal{F}_{4,2}(\phi)$ (orthogonal movement, full curve). Also shown is the spectrum of the video signal for perpendicular movement. The spectrum of $\mathcal{F}_{4,2}(\phi)$ does not have the nulls of $\mathcal{F}_{4,2}(\theta)$ and the slope is not as steep as the slope of the video spectrum.

seen that the PDS of the vertical-motion signal is closer to the shape of the video signal than was previously obtained for the $\mathcal{U}$ signal. However, the spectrum is still flatter than theory predicts. One probable explanation for the disparity rests with the assumption of the separability of $I(\alpha,\beta)$ that is inherent in the derivation of (17).

If the more fundamental relation of (15a) is used, we see that the PDS for the vertical u signal is

$$\mathcal{U}_{\Delta x}(\phi) = 2\{\mathfrak{I}[I(0,\beta)] - \mathfrak{I}[I(\Delta x,\beta)]\}. \quad (31)$$

If $I(\Delta x,\beta)$ is flatter than $I(0,\beta)$ rather than having the same shape, as separability requires, then $\mathfrak{I}[I(\Delta x,\beta)]$ will be more peaked at low frequencies than $\mathfrak{I}[I(0,\beta)]$. The difference spectrum $\mathcal{U}_{\Delta x}(\phi)$ would thus be flatter at lower frequencies than one would expect if separability, and hence (17), hold. This flattening of $I(\Delta x,\beta)$ relative to $I(0,\beta)$ does occur in the correlation function assumed in the next section. Also, there is strong evidence of this flattening in correlation measurements made by various workers [9], [10].

In summary, the measurements, by-and-large, support the theoretical predictions. The area in which the predictions failed were concerned with estimates of the slopes of power density spectra; in particular, the slope of the PDS of the frame-difference signal at low speeds and the slope of the PDS of the vertical-motion frame-difference signal.

IV. EVALUATION OF CORRELATION FUNCTIONS FOR MOVING IMAGES

The properties of the frame-difference correlation functions that were developed in Section II are best illustrated by example. In practical television systems, frame-to-frame changes in the video signal can arise from either changes in the scene, usually movement of one object, or from noise arising in the processing and/or transmission

system. By assuming appropriate image and noise correlation functions we can compute the correlation functions for the frame-difference signals arising from movement and from noise.

A. Correlation Function of a Moving Image

Correlation functions have been measured by a number of people [9]–[13]. Kretzmer and Capon used an optical technique and measured vertical and horizontal functions as well as measuring contours of constant correlation as a function of angle. Kretzmer used four scenes having very different amounts of detail; Capon used five. The correlation variable was the physical displacement of one transparency relative to the other; this could then be converted to horizontal or vertical picture elements.

O'Neal, Habibi and Wintz, and Allerot digitized the signal and used a computer to calculate the correlation function. O'Neal found the horizontal correlation function of the video signal generated by scanning, that is, as horizontal displacement increased one line wrapped around into the next line. The picture size was 100 × 100 samples. Correlation coefficients are also given for the seven spatially nearest samples in the previously transmitted signal.

Habibi and Wintz, using a 256 × 256 array calculated correlation functions in the horizontal, vertical, and diagonal directions for four pictures. Allerot used an interlaced television format of 208 × 250 picture elements and calculated correlation functions and contours of equal correlation. The contours were plotted in normalized horizontal units to bypass the difference in spacing between rows and columns of the television format.

By inspecting the results of these investigations there are a number of general observations one can make as follows.

1) The correlation function is a type of signature of the picture and gross deviations in the correlation function can usually be attributed to a specific characteristic of the picture (e.g., see [10]).

2) Correlation functions are mostly concave; a few approach being linear. Capon shows but one horizontal correlation function which is convex in the region from 0 to 20 elements displacement.

3) The spatial correlation function is approximately circular. If there is strong directional structure in the picture this will distort the shape of the contours, stretching them in the direction of the structure.

4) The adjacent-element correlation varies from 0.99 for a low-detailed picture to 0.8 for a high-detailed picture with an average scene having a value of approximately 0.95. Bear in mind that the correlation coefficient for shifts of one or two elements is very much affected by the type of prefiltering that has taken place (see Fig. 9 and discussion later in this section).

Approximating the correlation function by an exponential of the form $\exp\left[-(k_1\alpha^2 + k_2\beta^2)^{1/2}\right]$ provides a close fit to many functions. The more usual approximation is the separable function $\exp(-k_1 \mid \alpha \mid) \exp(-k_2 \mid \beta \mid)$

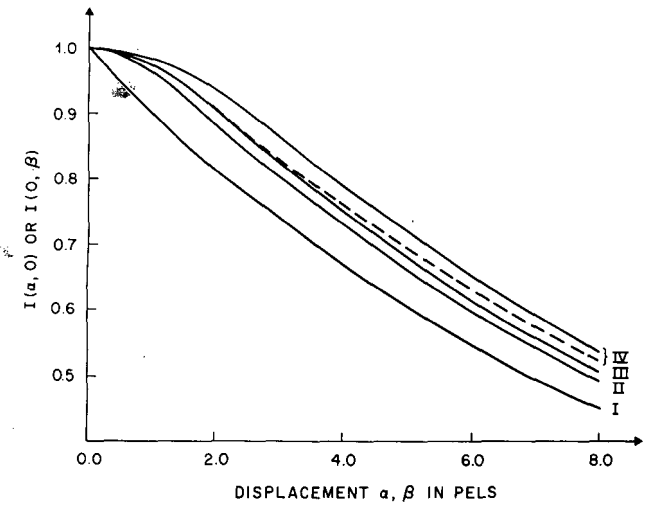

Fig. 9. Correlation functions of the video signal $I(\alpha,\beta)$ in the spatial directions parallel to the direction of movement ($I(\alpha,0)$) and orthogonal to the direction of movement ($I(0,\beta)$). I—Function $\exp\left[-0.1(\alpha^2 + \beta^2)^{1/2}\right]$; II—$I(\alpha,0) = I(0,\beta)$ for stationary image after filtering with 2-D Gaussian filter having an attenuation of 3 dB at 1/2 bandwidth; III—$I(\alpha,0)$ when filtered image moves at a speed of 2 pef; IV—$I(\alpha,0)$ (full line) and $I(0,\beta)$ (dashed line) when filtered image moves at a speed of 4.0 pef.

[12]. The first approximation would produce constant correlation contours that are ellipsoidal while for the second approximation the contours would be diamond shaped. An inspection of the correlation contours will give support to either approximation in particular instances although the most common shape from the available results would be closer to ellipsoidal. We assume the circular image correlation function

$$I(\alpha,\beta) = \exp\left(-0.10(\alpha^2 + \beta^2)^{1/2}\right) \tag{32}$$

which is plotted in Fig. 9.

Let us regard (32) as the correlation function of the light distribution of a single frame falling on the target. As discussed in Section II-C, camera integration will change the shape of the correlation function in the presence of movement. Convolving the correlation function with the correlation function of the camera integration impulse response gives the correlation function of the image residing on the camera target [8]. This signal is then filtered by the beam scanning operation and subsequent electrical filtering which we have approximated by a symmetrical two-dimensional Gaussian filter that is 3 dB down at half-bandwidth.[5]

The correlation function after camera integration and two-dimensional Gaussian filtering has been numerically evaluated and is shown in Fig. 9. Movement is assumed to be in the x direction. The curve for $\Delta x = 0$ shows just the effect of the two-dimensional filtering. As the speed increases the correlation in the direction of movement also increases. There is also a smaller increase in correlation orthogonal to the direction of movement. That there is any increase at all is attributable to the inseparable nature of the correlation function of the stationary image.

[5] The bandwidth is defined by the sampling rate (i.e., BW = 1/2 sampling rate).

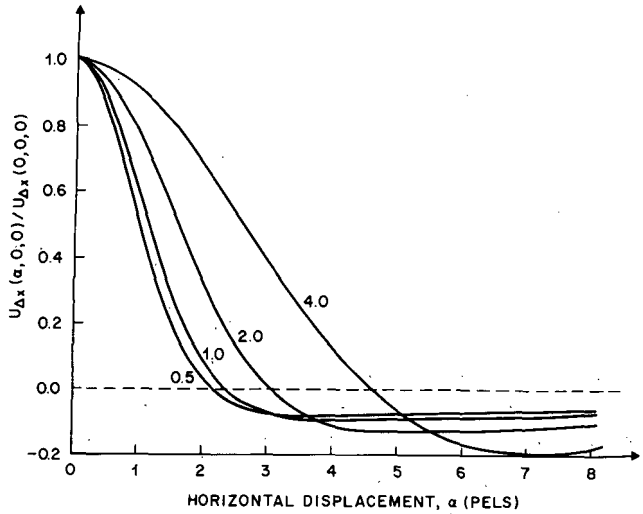

Fig. 10. Frame-difference correlation function $U_{\Delta x}(\alpha,0,0)$ (parallel to the direction of movement) as the speed increases from 0.5 to 4.0 pef. The calculations use the image correlation functions obtained after two-dimensional Gaussian filtering and camera integration of an image with an exponential correlation function $\exp(-0.1 \mid \rho \mid)$.

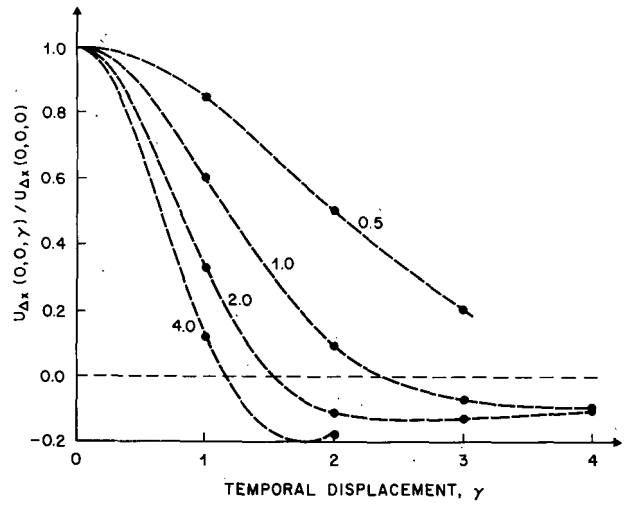

Fig. 11. Frame-difference correlation function $U_{\Delta x}(0,0,\gamma)$ in the temporal direction using the same image correlation functions as used in Fig. 10.

B. Correlation Functions of the Frame-Difference Signals Caused by Moving Images

Using the correlation functions for an image moving horizontally that were derived in the previous section, and using (10), we can obtain the correlation functions for the "moving" area frame-difference signals. [The functions for the "stationary" area frame-difference signals follow directly using (24).]

In Fig. 10 we have plotted the normalized "moving area" frame-difference correlation functions in the horizontal direction, i.e., parallel to the direction of movement. As expected the correlation function is speed dependent, the correlation between adjacent pels increasing rapidly with speed. The curves all have a region of negative correlation, and the depth of this negative lobe is seen to increase with speed.

These curves can also be used to obtain the temporal correlation function of the frame-difference signal, since by substitution in (10),

$$U_{\Delta x}(0,0,\gamma T) = U_{\Delta x}(\gamma \Delta x,0,0). \qquad (33)$$

If we replot the curves of Fig. 10 using the relation given in (33) we obtain the curves shown in Fig. 11. Obviously, there is a fairly high level of correlation between frames at low speeds, but the correlation decreases with increasing speed. This effect is very evident in Fig. 12 where we have plotted the correlation coefficient for adjacent frames as a function of speed.

The "moving area" frame-difference correlation functions in the vertical direction, i.e., perpendicular to the direction of motion, are shown in Fig. 13. At all speeds considered here, the correlation in the frame-difference signal in the vertical direction is greater than in either the horizontal or the temporal direction. Note also that in the

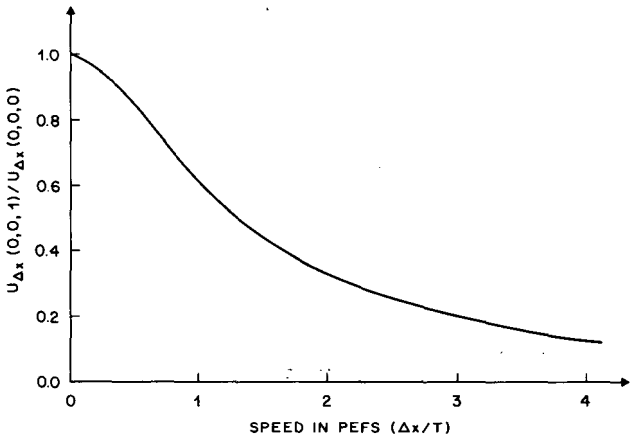

Fig. 12. Correlation between adjacent frames of the frame-difference signal as a function of speed using the same correlation functions as used in Fig. 10.

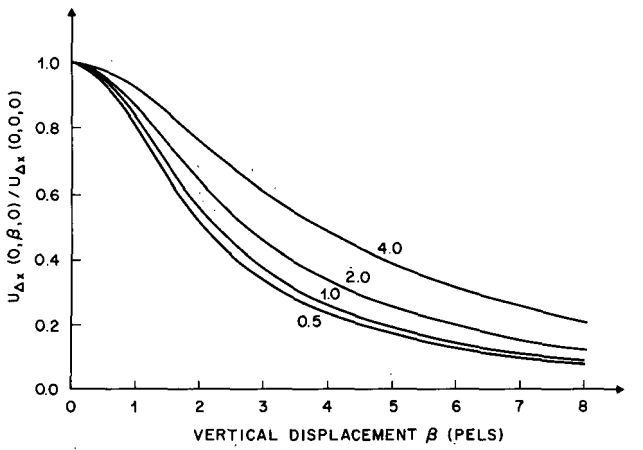

Fig. 13. Frame-difference correlation function $U_{\Delta x}(0,\beta,0)$ (in the spatial direction orthogonal to the direction of movement) using the same correlation functions as used in Fig. 10. There is no region of negative correlation contrary to the results for $U_{\Delta x}(\alpha,0,0)$ (Fig. 10) and $U_{\Delta x}(0,0,\gamma)$ (Fig. 11).

vertical direction there are no regions of negative correlation.

In order to give the reader a better feeling for the shape of the correlation functions in two dimensions and for how the shape changes with speed we have made the contour plots shown in Fig. 14. As the speed increases the contours for larger correlation values become more nearly circular.

V. CORRELATION OF THE FRAME-DIFFERENCE SIGNAL ARISING FROM NOISE

In detecting the presence of movement in pictures one invariably works with noisy signals. This noise may arise in any one of a number of ways and have many different properties, but in this study we will consider only additive noise which is uncorrelated with the picture. Suffixes n, N, and $\mathfrak{N}$ will be used to distinguish the noise waveform, correlation functions, and power spectra, respectively, from the corresponding signal quantities. Let the noise correlation function be

$$IN(\alpha,\beta,\gamma T) = \begin{cases} IN(\alpha,\beta), & \gamma = 0 \\ 0, & \gamma \neq 0 \end{cases} \tag{34}$$

that is, although the noise waveform in (x,y,jT) may be correlated within the frame, it is uncorrelated from frame-to-frame. Thus the relationship of (1) does not hold and consequently we cannot substitute (34) into (9) and (22) but must derive expressions for UN and FN without using (1). Considering the "moving" area first

$$\begin{aligned} UN(\alpha,\beta,\gamma T) = {} & \langle\{in(x,y,jT) - in[x,y,(j-1)T]\} \\ & \cdot\{in[x-\alpha, y-\beta, (j-\gamma)T] \\ & - in[x-\alpha, y-\beta, (j-\gamma-1)T]\} \end{aligned} \tag{35}$$

which, in a similar manner to (8), gives

$$\begin{aligned} UN(\alpha,\beta,\gamma T) = {} & 2IN(\alpha,\beta,\gamma T) - IN[\alpha,\beta,(\gamma+1)T] \\ & - IN[\alpha,\beta,(\gamma-1)T]. \end{aligned} \tag{36}$$

Substituting (34) in (36) gives

$$\begin{aligned} & UN(\alpha,\beta,\gamma T) \\ & = IN(\alpha,\beta)\{2DEL(\gamma T) - DEL[(\gamma+1)T] \\ & \quad - DEL[(\gamma-1)T]\} \end{aligned} \tag{37}$$

where

$$DEL(x) = \begin{cases} 1, & \text{if } x = 0 \\ 0, & \text{otherwise.} \end{cases} \tag{38}$$

Thus

$$UN(\alpha,\beta,0) = 2IN(\alpha,\beta) \tag{39}$$

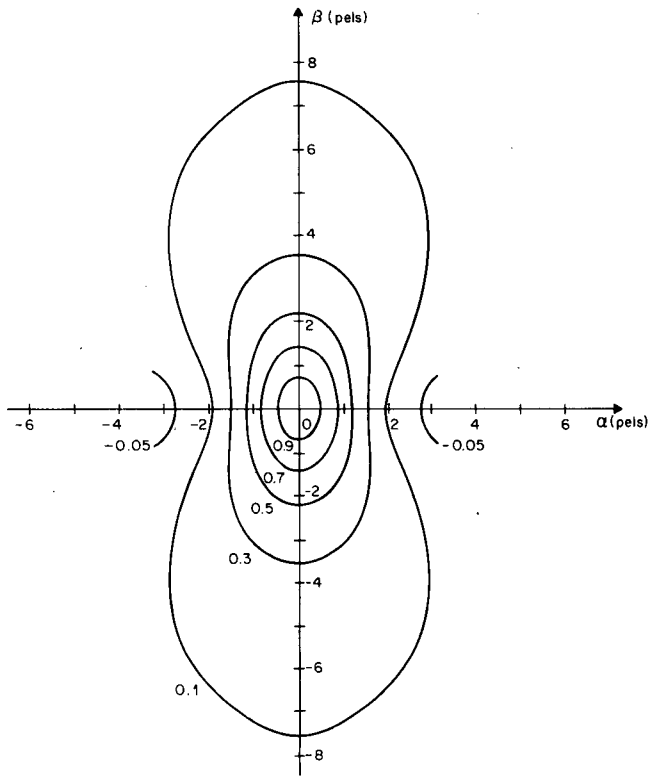

Fig. 14. Contours of constant correlation in the spatial plane using the same correlation functions as used in Fig. 10 for a speed of 1 pef. At low speeds correlation is much higher orthogonal to the direction of movement.

and hence the correlation function, normalized in the temporal direction is

$$\frac{UN(\alpha,\beta,\gamma T)}{UN(\alpha,\beta,0)} = \begin{cases} 1, & \text{if } \gamma = 0 \\ -1/2 & \text{if } \gamma = \pm 1 \\ 0, & \text{otherwise.} \end{cases} \tag{40}$$

The form of the correlation is shown in Fig. 15.

We saw previously that the "stationary" area frame-difference signal due to movement was not a stationary random process. Because the noise waveform is uncorrelated from frame to frame, however, the frame difference of the noise will be wide-sense stationary and we can calculate $FN(\alpha,\beta,\gamma T)$. Now

$$fn_\delta(x,y,jT) = in(x,y,jT) - in(x,y,j_0T) \tag{41}$$

with $j_0 = j - \delta$, where j_0 denotes the reference frame and δ denotes the number of frames between the reference frame and the current frame j. Also,

$$\begin{aligned} & fn_{\delta-\gamma}[x-\alpha, y-\beta, (j-\gamma)T] \\ & \quad = in[x-\alpha, y-\beta, (j-\gamma)T] \\ & \quad\quad - in(x-\alpha, y-\beta, j_0T) \end{aligned} \tag{42}$$

but note that we are only interested in values of γ less than δ, otherwise the first term in (42) will refer to a frame prior to the reference frame. Now

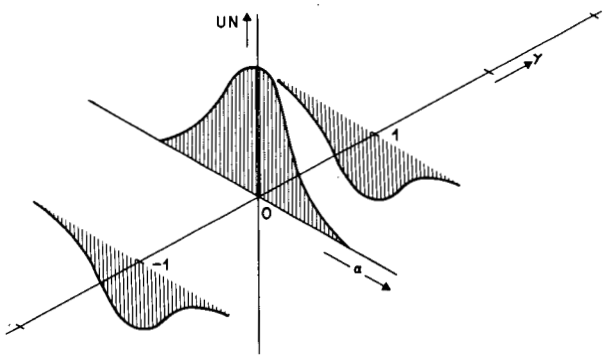

Fig. 15. Correlation function of frame-difference noise $UN(\alpha,\gamma)$ assuming no correlation of the noise from frame to frame and an arbitrary correlation function within the frame.

$$FN_\delta(\alpha,\beta,\gamma T) = \langle fn_\delta(x,y,jT) \cdot fn_{\delta-\gamma}[x-\alpha, y-\beta, (j-\gamma)T]\rangle \quad (43)$$

and after substituting (42) in (43) and using (34) we get

$$FN_\delta(\alpha,\beta,\gamma T) = IN(\alpha,\beta) \cdot [1 + DEL(\gamma T) - DEL((\gamma-\delta)T)]. \quad (44)$$

Now

$$FN_\delta(\alpha,\beta,0) = 2IN(\alpha,\beta) \quad (45)$$

and hence the temporally normalized correlation function is

$$\frac{FN_\delta(\alpha,\beta,\gamma T)}{FN_\delta(\alpha,\beta,0)} = \begin{cases} 1, & \text{if } \gamma = 0 \\ 0, & \text{if } \gamma = \delta \\ 1/2, & \text{otherwise.} \end{cases} \quad (46)$$

The form of the function is shown in Fig. 16.

Thus, on the basis of the above analysis, the frame-difference signal due to noise will have a negative temporal correlation in a "moving" area and a positive temporal correlation in a stationary area. This difference in the correlation arises from the fact that in the "moving" area the image function that is common to the two frame difference functions appears with differing sign, whereas in the "stationary" area the common image function has the same sign.

The difference in the moving area and stationary area noise signals is partially exploited in the movement detector described in [6]. In a type of decision-feedback configuration, areas previously detected as moving are low-pass filtered in the temporal direction; the filter is switched out in "stationary" areas.

VI. SUMMARY

In a conditional replenishment interframe encoder only information about the "moving" or changing area is transmitted. In a realistic environment, separation of the

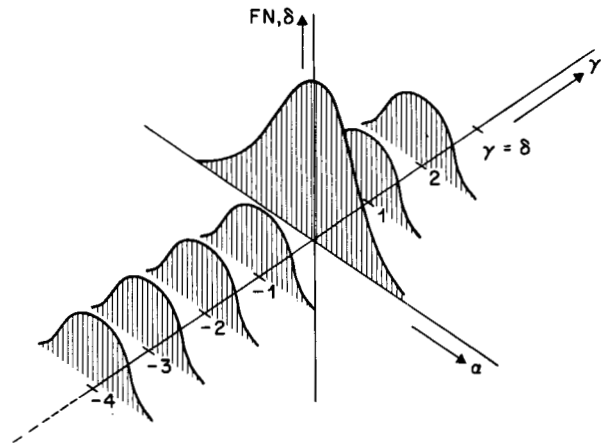

Fig. 16. Correlation function of frame-difference noise $FN_\delta(\alpha,\gamma)$ assuming no correlation of the noise from frame to frame and an arbitrary correlation function within the frame.

frame-to-frame changes caused by movement from those caused by noise is a difficult problem. A description of the properties of the frame-difference signals caused by movement and by noise will assist in its solution.

Two types of frame-difference signals occur in conditional replenishment encoders: those from "moving" areas that are continuously updated from frame to frame, and those from "stationary" areas that have not been updated for δ frames, $\delta > 1$. Neglecting camera integration, the spatial properties of a frame-difference signal arising from a "stationary" area moving at velocity $\Delta p_1/T$ will be the same as those from a "moving" area moving at velocity $\Delta p_2/T$ provided that $\Delta p_2 = \delta \Delta p_1$. The temporal properties of the two types of frame-difference signal are different, particularly in regard to the frame differences caused by noise.

Expressions for the spatial and temporal correlation functions and power density spectra of the "moving" and "stationary" (spatial only) area frame-difference signals have been developed for the case of uniform linear motion of an infinite image field. In order to compare the predicted power density spectra with spectra obtained using a video signal, the expressions for the power density spectra were modified to include the effect of camera integration.

The measured spectra, by-and-large, support the following theoretical predictions.

1) The video spectra showed clear evidence of camera integration at the higher speeds.

2) At slow speeds the power density spectra of the frame-difference signal is essentially flat. An expected 10 dB/decade fall was not observed.

3) The increase in the power of the frame-difference signal at low frequencies with every factor of two increase in speed was predicted to be 6 dB and was found to be 7 dB.

4) Predicted nulls in the power density spectra measured in the direction of motion were observed and were particularly pronounced in the "stationary" area frame-difference signal where the masking action of the camera integration is reduced.

5) Spectra measured at right angles to the direction of motion showed no nulls, as expected. The spectra, however, were not scaled replicas of the video spectra as predicted assuming separability of the latter. It was argued that this assumption was probably invalid for the test image.

In order to give tangible meaning to the expressions for the frame-difference correlation functions we evaluated them using a circularly symmetric, exponential correlation function that had undergone Gaussian spatial filtering and camera integration. The following properties were observed.

1) The correlation function of the frame-difference signal is highly speed dependent, the spatial correlation increasing rapidly with speed.

2) The correlation function in the direction of motion has a negative lobe.

3) The correlation between corresponding pels in adjacent frames is high at low speeds, but this correlation decreases rapidly with increasing speed.

4) The correlation function spatially perpendicular to the motion is greater than in the parallel or temporal directions.

5) As the speed increases the contours for the larger correlation values change from elliptical to almost circular.

6) Although not dealt with analytically, it should be noted that the frame-difference signal due to movement in a "stationary" area will increase steadily from frame-to-frame. Obviously, such a signal will have a high temporal dependence.

In order to study the correlation of the frame-difference signals arising from noise that is uncorrelated from frame to frame, new expressions were derived. Using these expressions it was found that the frame-difference signal due to noise will have a negative temporal correlation in a "moving" area and a positive temporal correlation in a "stationary" area.

In summary, the properties of the frame-difference signals arising in conditional replenishment encoders have been examined in some detail. The insights provided by this examination should assist in the design of movement detectors.

ACKNOWLEDGMENT

The assistance of K. A. Walsh in obtaining the experimental results is gratefully acknowledged. The comments of B. G. Haskell were most helpful in clarifying the analytic sections.

REFERENCES

[1] R. F. W. Pease and J. O. Limb, "Exchange of spatial and temporal resolution in television coding," *Bell Syst. Tech. J.*, vol. 50, pp. 191–201, Jan. 1971.
[2] J. C. Candy, M. A. Franke, B. G. Haskell, and F. W. Mounts, "Transmitting television as clusters of frame-to-frame differences," *Bell Syst. Tech. J.*, vol. 50, pp. 1889–1919, July–Aug. 1971.
[3] B. G. Haskell, F. W. Mounts, and J. C. Candy, "Interframe coding of videotelephone pictures," *Proc. IEEE (Special Issue on Digital Processing)*, vol. 60, pp. 792–800, July 1972.
[4] D. J. Connor, B. G. Haskell, and F. W. Mounts, "A frame-to-frame PICTUREPHONE® coder for signals containing differential quantizing noise," *Bell Syst. Tech. J.*, vol. 52, pp. 35–51, Jan. 1973.
[5] F. Rocca, "Television bandwidth compression utilizing frame-to-frame correlation and movement compensation," in *Picture Bandwidth Compression*, T. S. Huang and O. J. Tretiak, Ed. New York: Gordon and Breach, 1971, pp. 675–693.
[6] J. O. Limb, R. F. W. Pease, and K. A. Walsh, "Combining intraframe and frame-to-frame coding for television," *Bell Syst. Tech. J.*, vol. 53, July–Aug. 1974.
[7] A. J. Seyler, "Probability distributions of television frame differences," *Proc. IREE (Aust.)*, pp. 355–366, Nov. 1965.
[8] S. J. Mason and H. J. Zimmermann, *Electronic Circuits, Signals, and Systems*. New York: Wiley, 1960, p. 344.
[9] E. R. Kretzmer, "Statistics of television signals," *Bell Syst. Tech. J.*, vol. 31, pp. 751–763, July 1952.
[10] J. Capon, "Bounds to the entropy of television signals," Mass. Inst. Technol. Res. Lab. Electron., Cambridge, Tech. Rep. 296, May 25, 1955.
[11] J. B. O'Neal, Jr., "Predictive quantizing systems (differential pulse code modulation) for the transmission of television signals," *Bell Syst. Tech. J.*, vol. 45, pp. 689–721, May–June 1966.
[12] A. Habibi and P. A. Wintz, "Linear transformations for encoding 2-dimensional sources," School Elec. Eng., Purdue Univ., Lafayette, Ind., Rep. TR-EE, 70-2, Mar. 1970.
[13] R. J. Allerot, "Autocorrelation studies of typical PICTUREPHONE® scenes," unpublished memo., 1971.

Denis J. Connor was born on June 29, 1940. He received the B.A.Sc., M.A.Sc., and Ph.D. degrees from the University of British Columbia, Vancouver, B. C., Canada, in 1963, 1965, and 1969, respectively.

In 1969 he joined Bell Laboratories, Holmdel, N. J., where he worked on techniques for efficiently encoding television signals. He moved to Bell-Northern Research in Ottawa, Ont., Canada, in 1973 where he heads the Digital Signal Processing Systems Department. In parallel with this, he holds an appointment as a Professor in the Institut National de la Recherche Scientifique/Telecom, a research and educational institute established jointly by Bell-Northern Research and the University of Quebec, Quebec, P. Q., Canada.

★

John O. Limb (SM'72), for a photograph and biography please see page 820 of the June 1974 issue of this TRANSACTIONS.